Clinically, CFTD patients show generalized muscle hypotonia and weakness from infancy, multiple joint contractures, scoliosis, long thin face, and high arched palate. Approximately 30% of individuals with CFTD have mild-to-severe respiratory involvement. Cardiac involvement is seen in less than 10% of affected individuals [6,7]. Six causative genes for CFTD have been identified: *ACTA1* [8], *TPM3* [9], *RYR1* [10], *TPM2* [11], *MYH7* [12] and *SEPN1* [13] encoding α-skeletal actin, α-tropomyosin slow, ryanodine receptor type 1, β-tropomyosin, slow β-myosin heavy chain and selenoprotein N1, respectively.

In this study, we genetically screened CFTD patients for mutations in *LMNA*. We also re-evaluated clinical and pathological findings in patients previously diagnosed as having LMNA-myopathy to ascertain whether these patients have features similar to those of CFTD.

2. Materials and methods

All clinical materials used in this study were obtained for diagnostic purposes with written informed consent. This work was approved by the Ethics Committee of the National Center of Neurology and Psychiatry (NCNP).

2.1. Patients

We examined 80 unrelated muscle biopsies from the NCNP muscle repository. All specimens were from patients who had been diagnosed as having CFTD based on pathological findings as well as clinical features. All cases satisfied the pathological criteria for CFTD; mean type 1 fiber diameter is at least 12% smaller than the mean type 2 fiber diameter, with no structural abnormalities such as nemaline bodies, cores, and increased number of fibers with internal nuclei. In addition, we re-evaluated muscle pathology findings from 23 unrelated patients who had previously been diagnosed as having LMNA-myopathy. We chose genetically confirmed CFTD patients including 7 with *ACTA1* mutation and 2 with *TPM3* mutation for comparison of clinicopathological features. Clinically, all of the patients including in this study had muscle weakness and/or hypotonia from the preschool years (onset age; <6 years).

2.2. Mutation analysis

Genomic DNA was extracted from peripheral lymphocytes or frozen muscle specimens using standard techniques. For mutation screening of *LMNA*, *ACTA1* and *TPM3*, all exons and their flanking intronic regions were amplified by PCR and directly sequenced using an ABI PRISM 3100 automated sequencer (PE Applied Biosystems, Foster City, CA). Primer sequences are available on request.

2.3. Histochemical analysis of biopsied muscles

Biopsied skeletal muscles were frozen with isopentane cooled in liquid nitrogen. Serial frozen sections, 10 μm in thickness, were stained employing histochemical methods including hematoxylin and eosin (H&E), modified Gomori-trichrome (mGT), NADH-tetrazolium reductase (NADH-TR), and ATPases (pH 10.6, pH 4.6 and pH 4.3). For each muscle specimen, the mean fiber diameter was calculated by obtaining the shortest anteroposterior diameters of 100 type 1 and type 2 (A + B) fibers each using ATPase stains. Fiber size disproportion (FSD) was computed as; difference between type 2 fiber diameter (mean) and type 1 fiber diameter (mean) divided by type 2 fiber diameter (mean) × 100%. To obtain muscle fiber size information for age-matched controls, a total of 18 muscle specimens with minimal pathological changes from each age were examined.

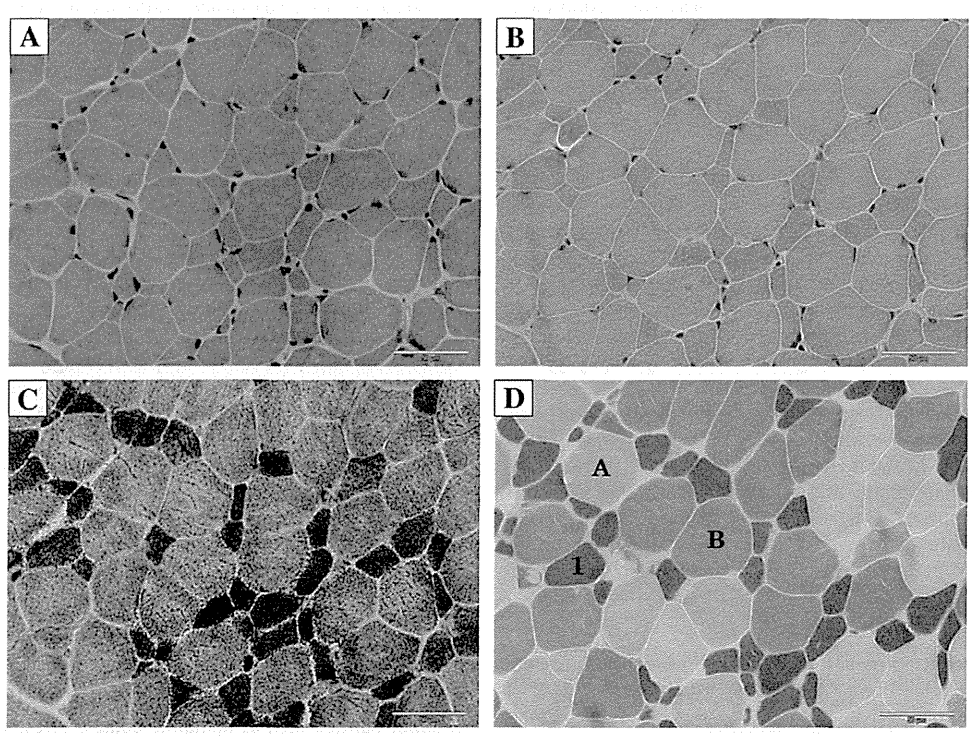

Fig. 1. Muscle biopsy from Patient 1 taken at age 4 years. (A) H&E stain shows marked variation in fiber size with neither fiber necrosis nor regeneration. (B) No nemaline bodies or cytoplasmic inclusions are revealed by mGT stain. On NADH-TR, intermyofibrillar networks are well organized. (D) On ATPase (pH 4.6), type 2A (A) and 2B (B) fibers are larger than type 1 (1) fibers. Bar = 50 μm.

Table 1
Histological features of LMNA-myopathy patients with FTD, CFTD patients with *ACTA1* and *TPM3* mutations.

Patient No.	Muscle Biopsied	Age at Biopsy	Type 1			Type 2A			Type 2B			Type 2C	%FSD	Mutation
			%	Mean Diameter (μM)	SD	%	Mean Diameter (μM)	SD	%	Mean Diameter (μM)	SD			
LMNA mutation														
1	Biceps	4y	52	16.5	5.0	30	39.1	5.3	18	37.1	7.5	0	57	c.367_369delAAG (p.K123del)
2	Quadriceps	2y	48	20.8	3.7	33	24.1	4.2	19	23.8	4.8	0	13	c.99_101delGGA (p.E33del)
3	NA	2y	38	28.6	7.7	50	36.3	4.4	7	31.3	10.5	5	15	c.1583C>A (p.T528K)
4	Biceps	4y	32	22.1	5.9	52	31.2	5.2	15	28.2	5.3	1	25	c.1357C>T (p.R453W)
5	Biceps	4y	56	21.6	5.6	32	40.0	5.8	10	34.0	8.4	2	42	c.1357C>T (p.R453W)
6	Biceps	5y	60	27.5	7.4	28	33.2	7.9	8	29.8	6.3	4	15	c.907T>C (p.S303P)
ACTA1 mutation														
1	Biceps	4y	73	14.5	3.7	26	17.8	3.7	1	–	–	0	18	c.16G>A (p.E6K)
2	Quadriceps	0y6m	60	11.9	3.1	10	18.0	2.8	20	18.8	2.8	10	35	c.143G>T (p.G48C)
3	Quadriceps	0y7m	60	6.8	1.6	29	11.5	2.1	3	–	–	8	44	c.143G>T (p.G48C)
4	NA	0y1m	52	5.6	1.5	28	14.4	2.0	12	10	2.8	8	57	c.668 T>C (p.L223P)
5	Biceps	10y	70	11.9	2.3	27	17.2	3.2	2	–	–	1	31	c.682G>C (p.E228Q)
6	Biceps	0y9m	62	10.5	2.8	23	17.2	2.8	10	18.8	2.8	5	42	c.981T>A (p.M326K)
7	Biceps	0y10m	72	12.0	1.8	22	19.5	3.5	3	–	–	3	36	c.1000C>T (p.P332S)
TPM3 mutation														
1	Biceps	0y5m	56	9.0	2.4	44	24.4	3.2	0	–	–	0	63	c.502C>T (p.R168C)
2	Biceps	0y6m	58	9.7	2.0	20	17.9	2.5	16	17.1	2.4	6	45	c.502C>T (p.R168C)

SD = standard deviation; NA = data not available; dash = not applicable.

2.4. Electron microscopic observation

Muscle specimens were fixed with 2% glutaraldehyde in 0.1 M cacodylate buffer. After shaking with a mixture of 4% osmium tetroxide, 1.5% lanthanum nitrate, and 0.2 M s-collidine for 2–3 h, samples were embedded in epoxy resin. Semi-thin sections (1 μm-thickness) were stained with toluidine blue. Ultrathin sections, 50 nm in thickness, were stained with uranyl acetate and lead citrate, and then examined

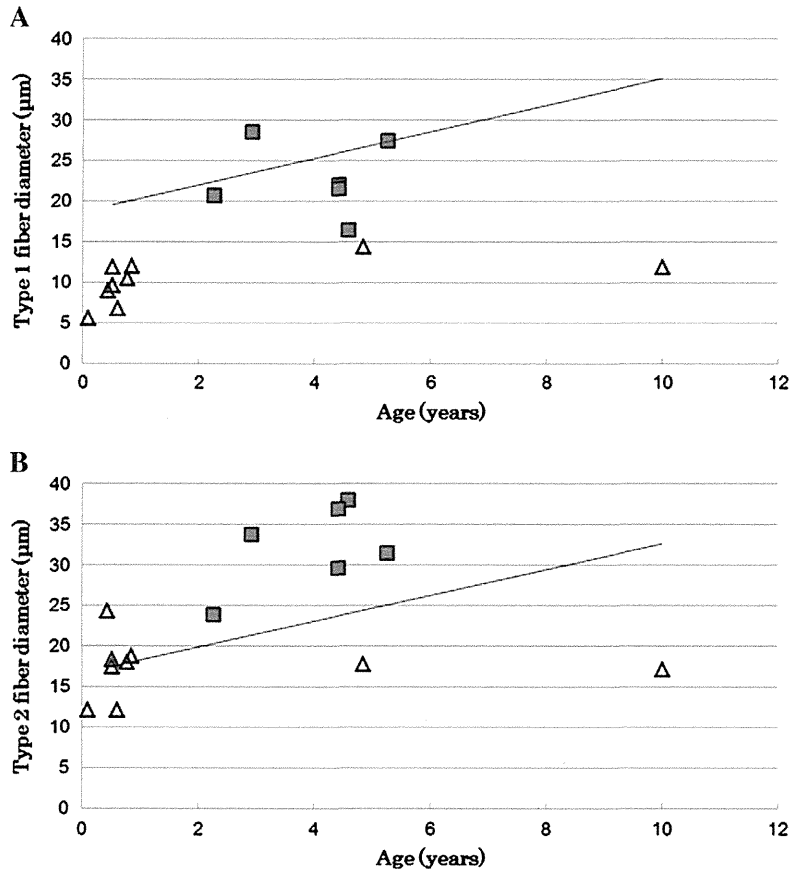

Fig. 2. Composition of mean muscle fiber diameter in each patient. (A) Mean diameters of type 1 fibers, (B) Mean diameters of type 2 fibers. Filled squares represent LMNA-myopathy with FTD, open triangles show CFTD with *ACTA1* or *TPM3* mutations, and the solid line indicates the mean fiber diameter of age-matched controls for children at various ages taken from biopsies classified as normal. CFTD with *ACTA1* and *TPM3* mutations show type 1 fiber atrophy whereas LMNA-myopathy with FTD shows type 2 fiber hypertrophy.

Table 2
Clinical and pathological summary of LMNA-myopathy patients with FTD.

Patient No	Sex	Age at Diagnosis (yr)	Age at biopsy (yr)	Pathological diagnose	Age at walk (mo)	Hypotonia	High arched palate	Respiratory involvement	Cardiac symptoms	Other presenting signs/Symptoms (age/yr)	CK (IU/L)	FSD (%)
1	M	16	4	CFTD	12	Yes	No	No	AV-b, ICRBBB (16 yr)	Joint contractures (4)	330	57
2	M	4	2	CFTD	14	Yes	No	No	No	Joint contractures (2) Dropped head (4) Rigid spine (4)	367	13
3	M	10	2	MD	15	Yes	No	No	No	Joint contractures (2) Rigid spine (8)	1098	15
4	F	4	4	MD	12	Yes	No	No	No	No	1408	25
5	F	13	4	MD	14	No	No	No	No	Lordosis (4) Joint contracture (6) Rigid spine (10)	1985	42
6	F	5	5	MD	18	No	No	No	No	No	303	15

MD; muscular dystrophy, AV-b; atrioventricular block, IRBBB; incomplete right bundle-branch block, PAF; paroxysmal atrial fibrillation.
Patients 1 and 2 were initially diagnosed as having CFTD. Patients 3 to 7 were genetically confirmed to have LMNA-myopathy with FTD. None of the patients had a high arched palate and/or respiratory involvement. Serum creatine kinase (CK) was mildly elevated in all patients.

under a tecnai spirit transmission electron microscope (FEI, Japan) at 120 kV.

2.5. Statistical analysis

All data are presented as means ± SD. Comparisons among groups were made using Student's *t* test and analysis of variance (ANOVA). A difference was considered to be statistically significant at a p value less than 0.05.

3. Results

3.1. Mutation analysis

Among the 80 unrelated patients who were diagnosed as having CFTD based on clinical and pathological findings, a heterozygous *LMNA* mutation was identified in two; a previously reported c.367_369delAAG (p.Lys123del) in Patient 1 and a novel c.99_101delGGA (p.Glu33del) in Patient 2 [14]. *ACTA1* mutations found in the 7 CFTD patients were c.16G>A (p.Glu6Lys), c.142G>T (p.Gly48Cys), c.668T>C (p.Leu223Pro), c.682G>C (p.Glu228Gln), c.980T>A (p.Met327Lys), and c.1000C>T (p.Pro334Ser). Two CFTD patients had the same heterozygous c.502C>T (p.Arg168Cys) mutation in *TPM3*. The novel mutations of *LMNA* c.99_101delGGA (p.Glu33del) and *ACTA1* c.980T>A (p.Met327Lys), were not found in either 100 Japanese control chromosomes or the dbSNP and 1000 Genomes databases.

3.2. Histological findings

Histologically, type 1 fiber predominance (more than 55% of type 1 fibers) and type 2B fiber deficiency (less than 5% of type 2B fibers) were observed in 61% and 28%, respectively, of our 80 CFTD cohort. These results are consistent with those of a previous report [7].

Two patients with *LMNA* mutations showed a marked difference in the sizes of type 1 and type 2 fibers, resulting in FSD of 57% and 13%, respectively (Fig. 1). Neither type 1 fiber predominance nor type 2B fiber deficiency was seen (Table 1).

Re-evaluation of genetically confirmed LMNA-myopathy revealed that 4 of 23 patients (17%) had fiber type disproportion (FTD). Their FSD was ranged from 15 to 42%. All 4 patients with FTD also showed some necrotic and/or regenerating fibers in their muscle biopsy and had a diagnosed of muscular dystrophy. These 4 patients with FTD had 3 different mutations. Two mutations of c.1583C>A (p.Thr528Lys) and c.1357C>T (p.Arg453Trp) have already been reported [15,16], whereas the c.907 T>C (p.Ser303Pro) mutation was not reported previously. These mutations were distributed in both central rod and tail domains, but not in the head domain (Table 1).

To clarify whether LMNA-myopathy patients with FTD have specific pathological findings different from those affecting CFTD muscles with known gene mutations, we carefully re-evaluated the muscle pathologies of the 6 LMNA-myopathy patients with FTD, 7 CFTD patients with *ACTA1* mutations, and 2 CFTD patients with *TPM3* mutations. FSD in LMNA-myopathy with FTD, and in CFTD with *ACTA1* and *TPM3* mutations were calculated to be 27.8 ± 17.9% (mean ± SD), 37.7 ± 12.1%, and 54.1 ± 13.1%, respectively. No significant differences were seen in FSD among the 3 groups. We also compared fiber sizes among LMNA-myopathy with FTD, CFTD with *ACTA1* or *TPM3* mutations and age-matched controls. Surprisingly, CFTD with *ACTA1* and *TPM3* mutations showed type 1 fiber atrophy, whereas LMNA-myopathy with FTD showed type 2 fiber hypertrophy with lack of type 1 fiber atrophy (Fig. 2).

In this study, type 1 fiber predominance was seen in 86% of CFTD patients with *ACTA1* mutations and in 100% of those with *TPM3* mutations, but in only 33% of LMNA-myopathy patients with FTD. The percentage of type 1 fibers in LMNA-myopathy was calculated to be 44.6 ± 12.8 (mean ± SD), which was significantly lower than that in CFTD with *ACTA1* mutations (64.1 ± 7.1%) and that with *TPM3* mutations (57.0 ± 1.4%) ($p < 0.05$). Type 2B fiber deficiency was not seen in LMNA-myopathy with FTD (Tables 1, 3), whereas 4 of 7 (57%) patients with *ACTA1* mutations and one (50%) with *TPM3* mutation showed type 2B fiber deficiency.

On electron microscopic (EM) observations, nuclear changes are important pathological findings in skeletal muscles of LMNA-myopathy [4]. We examined the nuclear changes in Patients 2, 4 and 5 on EM, and found a few myonuclei showing abnormal shapes and chromatin disorganization (Fig. 3). Smaller nuclei arranged in a row, giving the appearance of a 'nuclear chain', were also seen (data not shown). However, nuclear abnormalities in patients who had LMNA-myopathy with

Table 3
Comparison of clinical and pathological information between LMNA-myopathy with FTD and CFTD with *ACTA1* and *TPM3* mutations.

Gene mutation	*LMNA*	*ACTA1*	*TPM3*
Number of patients	6	7	2
Onset	Infantile	at birth	< 2 months
Hypotonia	67% (4/6)	100% (7/7)	100% (2/2)
High arched palate	0% (0/6)	57% (4/7)	50% (1/2)
Respiratory involvement	0% (0/6)	57% (4/7)	0% (0/2)
Joint contracture	67% (4/6)	14% (1/7)	0% (0/2)
CK level (IU/L)	963 ± 662	53 ± 15	42 ± 16
Type 1 fiber predominance	33% (2/6)	86% (6/7)	100% (2/2)
Type 2B fiber deficiency	0% (0/6)	57% (4/7)	50% (1/2)

Type 1 fiber predominance and absence of type 2B fibers were common in CFTD caused by *ACTA1* or *TMP3* mutations. Type 2B fiber deficiency was not seen in LMNA-myopathy with FTD. Serum creatine kinase (CK) levels were significantly higher in LMNA-myopathy than in CFTD with *ACTA1* and *TPM3* mutations ($p < 0.05$).

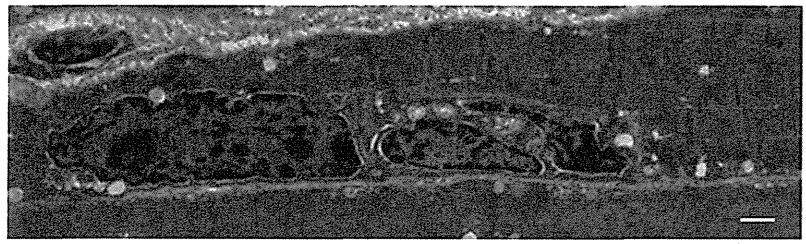

Fig. 3. Myonuclear shape changes in patient 2. Nuclear contours are irregular with a serpentine appearance. Bar = 1 μm.

FTD were milder and less frequent than previously reported for AD-EDMD and LGMD1B muscles [4].

3.3. Clinical findings

Table 2 summarizes the characteristics of the 6 LMNA-myopathy patients with FTD. Patients 1 and 2 were initially diagnosed as having CFTD, and the 4 remaining patients (patients 3 to 6) showed FTD together with dystrophic changes on muscle pathology. All patients had normal antenatal courses and uneventful births. All patients had started walking without delay, but showed a waddling gait and muscle weakness and/or hypotonia from the preschool years. None had a high arched palate or respiratory dysfunction. Four of the 6 (67%) patients had contractures of the ankles and/or elbows which had not been present at birth but appeared with age. Serum creatine kinase (CK) was mildly elevated in all patients.

Sixteen of the 78 (21%) CFTD patients with unknown cause had high CK levels (>200 IU/l), and four of these 16 showed a high arched palate and respiratory involvement.

4. Discussion

FTD can be seen in a single muscle biopsy from patients with several diseases including congenital myotonic dystrophy and centronuclear myopathy [17–20]. Here we identified 2 LMNA-myopathy among patients diagnosed as CFTD. We also found FTD in 17% of muscular dystrophy patients with LMNA mutations. These results suggest that FTD may not be rare in LMNA-myopathy. None of these patients had either a high arched palate or respiratory insufficiency, and serum CK levels were mildly elevated. Pathologically, FTD in LMNA-myopathy is associated with type 2 fiber hypertrophy with lack of type 1 fiber atrophy, whereas type 1 fiber atrophy is seen in CFTD with *ACTA1* or *TPM3* mutations. Unlike CFTD due to *ACTA1* or *TPM3* mutations, type 1 fiber predominance and type 2B fiber deficiency are absent in LMNA-myopathy. These results suggest that *LMNA* analysis should be performed in CFTD patients who has the clinical features such as no high arched palate, no respiratory insufficiency and high CKemia, and has pathological features such as type 2 fiber hypertrophy and lack of type 1 fiber atrophy, type 1 fiber predominance, and type 2B fiber deficiency.

LMNA-myopathy is categorized as muscular dystrophy, and mild necrotic and regenerating processes are usually seen. However, no dystrophic features can be seen as reported herein. Higher CK levels raise the possibility of LMNA-myopathy being dystrophic in nature. On the other hand, in our series, 16 of the 78 (21%) CFTD patients with unknown cause had high CKemia. This result suggests a difficulty in making a differential diagnosis between congenital myopathy and muscular dystrophy in some cases.

Clinically, respiratory insufficiency is common, reportedly being seen in 30% of CFTD patients [7], and in 73% of L-CMD patients [4]. However, 2 CFTD patients with *LMNA* mutations in this study showed no respiratory involvement. Furthermore, in CFTD associated with *LMNA* mutations, FTD is the only pathological abnormality, while prominent dystrophic and/or inflammatory changes are seen in L-CMD. There results suggest that CFTD is the milder form of early onset LMNA-myopathy.

Acknowledgments

This study was supported partly by Research on Intractable Diseases, Comprehensive Research on Disability Health and Welfare, and Applying Health Technology from the Ministry of Health Labour and Welfare; partly by Intramural Research Grant 23-5 for Neurological and Psychiatric Disorders of NCNP; and partly by JSPS KAKENHI Grant Numbers of 24390227 and 24659437.

References

[1] Emery AE. Emery-Dreifuss muscular dystrophy - a 40 year retrospective. Neuromuscul Disord 2000;10:228–32.
[2] Muchir A, Bonne G, van der Kooi AJ, et al. Identification of mutations in the gene encoding lamins A/C in autosomal dominant limb girdle muscular dystrophy with atrioventricular conduction disturbances (LGMD1B). Hum Mol Genet 2000;9:1453–9.
[3] Quijano-Roy S, Mbieleu B, Bönnemann CG, et al. De novo LMNA mutations cause a new form of congenital muscular dystrophy. Ann Neurol 2008;64:177–86.
[4] Park YE, Hayashi YK, Goto K, et al. Nuclear changes in skeletal muscle extend to satellite cells in autosomal dominant Emery-Dreifuss muscular dystrophy/limb-girdle muscular dystrophy 1B. Neuromuscul Disord 2009;19:29–36.
[5] Komaki H, Hayashi YK, Tuburaya R, et al. Inflammatory changes in infantile-onset LMNA-associated myopathy. Neuromuscul Disord 2011;21:563–8.
[6] Banwell BL, Becker LE, Jay V, et al. Cardiac manifestations of congenital fiber-type disproportion myopathy. J Child Neurol 1999;14:83–7.
[7] Clarke NF, North KN. Congenital fiber type disproportion - 30 years on. J Neuropathol Exp Neurol 2003;62:977–89.
[8] Laing NG, Clarke NF, Dye DE, et al. Actin mutations are one cause of congenital fiber type disproportion. Ann Neurol 2004;56:689–94.
[9] Clarke NF, Kolski H, Dye DE, et al. Mutations in TPM3 are a common cause of congenital fiber type disproportion. Ann Neurol 2008;63:329–37.
[10] Clarke NF, Waddell LB, Cooper ST, et al. Recessive mutations in RYR1 are a common cause of congenital fiber type disproportion. Hum Mutat 2010;31:E1544–50.
[11] Clarke NF, Waddell LB, Sie LT, et al. Mutation in TPM2 and congenital fiber type disproportion. Neuromuscul Disord 2012;22:955–8.
[12] Ortolano S, Tarrio R, Blanco-Arias P, et al. A novel MYH7 mutation links congenital fiber type disproportion and myosin storage myopathy. Neuromuscul Disord 2011;21:254–62.
[13] Clarke NF, Kidson W, Quijano-Roy S, et al. SEPN1: associated with congenital fiber-type disproportion and insulin resistance. Ann Neurol 2006;59:546–52.
[14] Keller H, Finsterer J, Steger C, et al. Novel c.367_369del LMNA mutation manifesting as severe arrythmias, dilated cardiomyopathy, and myopathy. Heart Lung 2012;41:382–6.
[15] Bonne G, Mercuri E, Muchir A, et al. Clinical and molecular genetic spectrum of autosomal dominant Emery-Dreifuss muscular dystrophy due to mutations of lamin A/C gene. Ann Neurol 2000;48:170–80.
[16] Brown CA, Lanning RW, McKinney KQ, et al. Novel and recurrent mutation in lamin A/C in patients with Emery-Dreifuss muscular dystrophy. Am J Med Genet 2001;102:359–67.
[17] Tominaga K, Hayashi YK, Goto K, et al. Congenital myotonic dystrophy can show congenital fiber type disproportion pathology. Acta Neuropathol 2010;119:481–6.
[18] Danon MJ, Giometti CS, Manaligod JR, Swisher C. Sequential muscle biopsy changes in a case of congenital myopathy. Muscle Nerve 1997;20:561–9.
[19] Shishikura K, Osawa M, Suzuki H, et al. Clinical variability of congenital myopathy with type 1 fiber atrophy: a long-term observation of three cases. Acta Paediatr Jpn 1994;36:186–93.
[20] Okamoto N, Toribe Y, Nakajima T, et al. A girl with 1p36 deletion syndrome and congenital fiber type disproportion myopathy. J Hum Genet 2002;47:556–9.

骨格筋チャネル病の最新知見
——ミオトニー症候群と周期性四肢麻痺を中心に

Update of the skeletal muscle channelopathies——myotonic syndromes and periodic paralysis

久保田智哉(写真)　高橋正紀
Tomoya KUBOTA[1,2] and Masanori P. TAKAHASHI[1]
大阪大学大学院医学系研究科神経内科学[1]，シカゴ大学生化学・分子生物学[2]

◎骨格筋にはさまざまなイオンチャネルが存在し，電気生理的活動を担っている．これらのチャネルの機能異常はミオトニー，麻痺，筋小胞体の障害などを主とする疾患の原因となり，骨格筋チャネル病と総称される．この骨格筋チャネル病にはチャネル遺伝子自体の変異による一次性と，他の原因によりチャネルの発現や機能が影響を受けて発症する二次性とがある．一次性のうち，ミオトニー症候群に関しては，Nav1.4チャネルによる疾患を中心に臨床診断，遺伝子変異同定，変異チャネル機能解析を通じて理解が深まっている．また，麻痺を主症状とする疾患については，電位感受性ドメインに生じる漏洩電流(gating pore電流)の発見により病態生理の解明に近づいている．一方，二次性については甲状腺中毒性周期性四肢麻痺の一部でKir2.6という新規原因チャネルが近年同定されたものの大部分は不明であり，複数の原因で構成される症候群と考えられ，さらなる研究がまたれる．

Key word：骨格筋，Naチャネル，ミオトニー，甲状腺中毒性，周期性四肢麻痺，gating pore電流

骨格筋細胞膜にはさまざまなイオンチャネルが存在し，骨格筋の電気的活動を担っている．これらのイオンチャネルの機能異常はミオトニーや麻痺といった症状を呈する疾患の原因となり，骨格筋チャネル病(以下，筋チャネル病)と総称される．

本稿ではまず筋チャネル病の広がりについて概説する．さらに，さまざまな遺伝子異常により生じる変異チャネルの機能異常がどのように筋チャネル病の病態生理へつながるか，最近の知見についてミオトニー症候群と周期性四肢麻痺を中心に述べる．

筋チャネル病の分類

筋チャネル病は“筋細胞膜の障害を主とする疾患”と“筋小胞体の障害を主とする疾患”に大別できる．“筋細胞膜の障害を主とする疾患”は臨床症状から，①ミオトニーが主症状の疾患，②麻痺症状が主症状の疾患，に大別できるが，症状が混在しはっきりと区別しがたい例も多い．また，イオンチャネル遺伝子自体の変異によるもの(一次性)と，他の原因によりイオンチャネルの発現や機能が影響を受けて発症するもの(二次性)とがある(図1)．

ミオトニーは臨床的には，随意的または叩打により誘発された筋収縮の弛緩遅延と定義される．その生理学的本態は筋細胞膜の異常な興奮性亢進である．このミオトニーを呈する疾患群を総称し，ミオトニー症候群とよぶ[1]．一次性ミオトニー症候群は非ジストロフィー性ミオトニー症候群(non-dystrophic myotonia)ともよばれるが，実際には筋萎縮を呈する症例も散見される．一方，麻痺症状の本態は筋細胞膜が脱分極した状態が続くことで起こる脱分極性麻痺であり，筋細胞膜異常興奮性による症状という点でミオトニー症候群と共通の病態を背景にもつ．

以下，筋チャネル病を分類に沿って概説する．

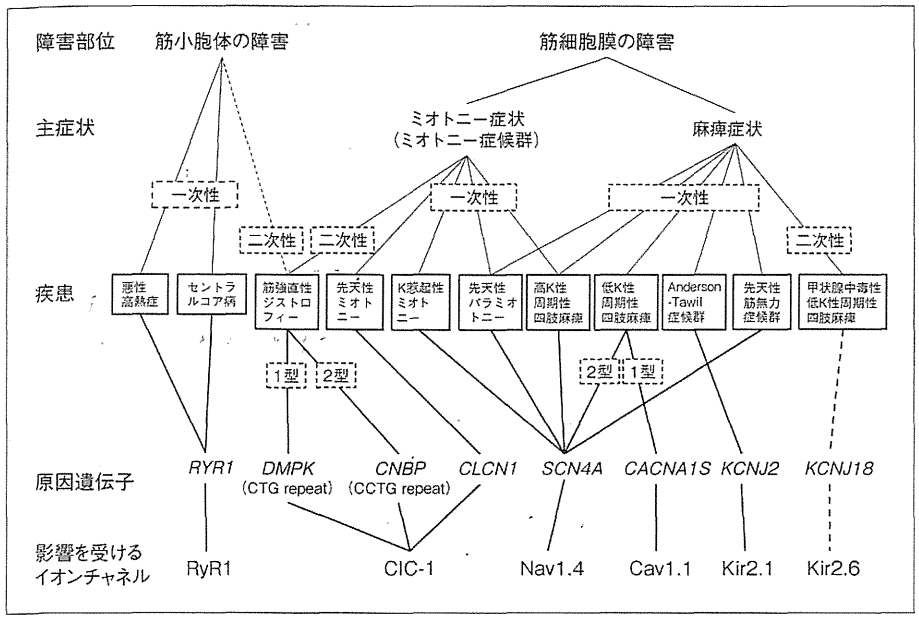

図 1　骨格筋チャネル病の分類

骨格筋チャネル病は“筋細胞膜の障害を主とするもの”と“筋小胞体の障害を主とするもの”に大別される．また前者は，ミオトニーを主症状とするもの，麻痺(筋無力症状)を主症状とするものに大別される．各疾患の原因遺伝子，原因となるチャネルを示す．破線は関連が示唆されているものを示す．

一次性筋チャネル病

1. ミオトニー症候群

① 骨格筋型Cl^-チャネル異常によるミオトニー

骨格筋型Cl^-チャネル(ClC-1)は7番染色体上にある*CLCN1*遺伝子にコードされている．2つのサブユニットからダイマーを形成するが，各サブユニットはプロトポアとよばれるイオン伝達経路を別々に形成し，Cl^-イオンを透過させる．

筋細胞膜には神経に比べてCl^-チャネルが豊富に存在し，その平衡電位は静止膜電位に近い．ClC-1は電位変化に対し比例してCl^-イオンを通す性質をもつため，膜電位を安定化させる効果をもつ．この点で，筋細胞の興奮性において，ClC-1は重要な役割を担う．ClC-1異常によるミオトニーはその機能低下・発現量の低下(loss of function)による．

先天性ミオトニー(myotonia congenita：MC；Thomsen病，Becker病)は，外眼筋，顔面筋や舌筋を含む全身の骨格筋にみられるミオトニーと筋肥大を特徴とする．ミオトニーは筋を繰り返し収縮させることにより軽減する(warm-up現象)．優性遺伝型をThomsen病，劣性遺伝型をBecker病とよぶ．Becker病のほうがThomsen病よりも重度となる傾向がある．優性遺伝形式でも発症する理由として，正常チャネルの機能に影響する優性陰性(dominant negative)変異によるとされている．

② 骨格筋型Naチャネル異常によるミオトニー

骨格筋型Naチャネル(Nav1.4)は17番染色体上にある*SCN4A*遺伝子にコードされている．Nav1.4は6つの膜貫通セグメント(S1～S6)をもつドメインが4つ(DⅠ～DⅣ)つながって構成される(図2-A)．各ドメインのS5とS6は1つのチャネルの穴(ポア)を形成する．S4は3アミノ酸ごとに正電荷をもつアミノ酸(アルギニンまたはリジン)が規則正しく並ぶ構造をもち，これらをgating chargeとよぶ．また，S1からS4までを総称して電位感受性ドメイン(VSD)とよぶ(図2，3)[2]．

カリウム(K)惹起性ミオトニー(potassium

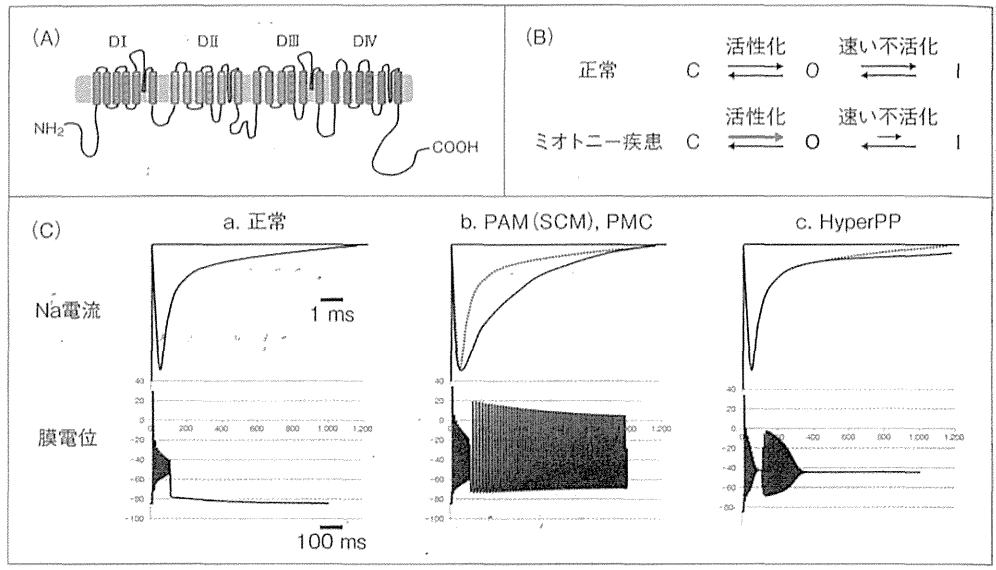

図 2　Nav1.4によるミオトニー症候群

A：Nav1.4チャネルを示す．実際にはこのNav1.4に，補完サブユニットであるβサブユニットが組み合わさって筋細胞膜上に存在すると考えられている．6回膜貫通セグメント(S1～S6)をもつ4つのドメイン(DⅠ～DⅣ)で構成される．S1～S4を電位感受性ドメイン(voltage sensing domain：VSD)，S5およびS6はポアドメインとよぶ．

B：Nav1.4の活性化しチャネルが開いた状態(O)，チャネルが閉じている状態(C)，不活化している状態(I)を模式的に示す．活性化が亢進，速い不活化が障害，あるいはその両方によりNav1.4は開いた状態(O)になりやすく，興奮性が亢進した状態となり，ミオトニー放電が生じる．

C：Nav1.4異常症の各疾患とチャネル機能異常の関係を示す．上段はNa電流を，下段はその機能異常をもとに筋細胞膜の電位変化のシミュレーションを示している．正常では筋細胞に電流が流れている間のみ活動電位が発生する(a)．Nav1.4の速い不活化が障害されている場合，Na電流の減衰が遅くなる(b上段)．このとき筋細胞膜は電流が流れたあとも自発的活動電位(myotonic discharge)が発生し，これがPAMやPMCの病型にあたる(b)．Nav1.4の遅い不活化が障害されている場合，Na電流が減衰しきらずに電流が流れつづける(c上段)．このとき，筋細胞膜は電流の流れたあとも活動電位が発生し，ついには脱分極性麻痺に至る．これがHyperPPの病型にあたる(c)．

aggravated myotonia：PAM)，先天性パラミオトニー(paramyotonia congenita：PMC)，高K性周期性四肢麻痺(hyperkalemic periodic paralysis：HyperPP)は同じ*SCN4A*遺伝子の変異で生じる疾患群である．ClC-1異常によるミオトニーはClC-1のloss of functionで生じるのに対し，上記3疾患は*SCN4A*変異によりNav1.4の機能がより興奮性亢進へと変化する(gain of function)ことにより生じる．Nav1.4には，①活性化しチャネルが開いた状態(O)，②チャネルが閉じている状態(C)，③不活化している状態(I)，がある(図2-B)．不活化状態はイオンを透過しないという点では閉じている状態と同様であるが，いかに脱分極させてもイオンが透過可能にはならないという点で異なる．不活化にはその時間経過から，速い不活化と遅い不活化のすくなくとも2種類がある．速い不活化は活動電位発生後の再分極に関与する．遅い不活化については数百msecから数sec以上の長い脱分極により生じる不活化状態で，複数の状態があると考えられているが，生理的意義も含めて詳細は不明な部分が多い．これらNav1.4の状態のうち，どの機能異常が筋細胞膜全体の興奮性にどのように影響するか，実験データをもとにしたコンピュータシミュレーションを用いて検討されてきており，上記3疾患と機能異常との関連が明らかになってきている[3](図2-C)．

PAM(SCM)：運動やカリウム経口摂取後の筋のこわばりを特徴とする．現在はNaチャネルミオトニー(sodium channel myotonia：SCM)とよぶべきと提唱されている[1]．軽症(myotonia fluc-

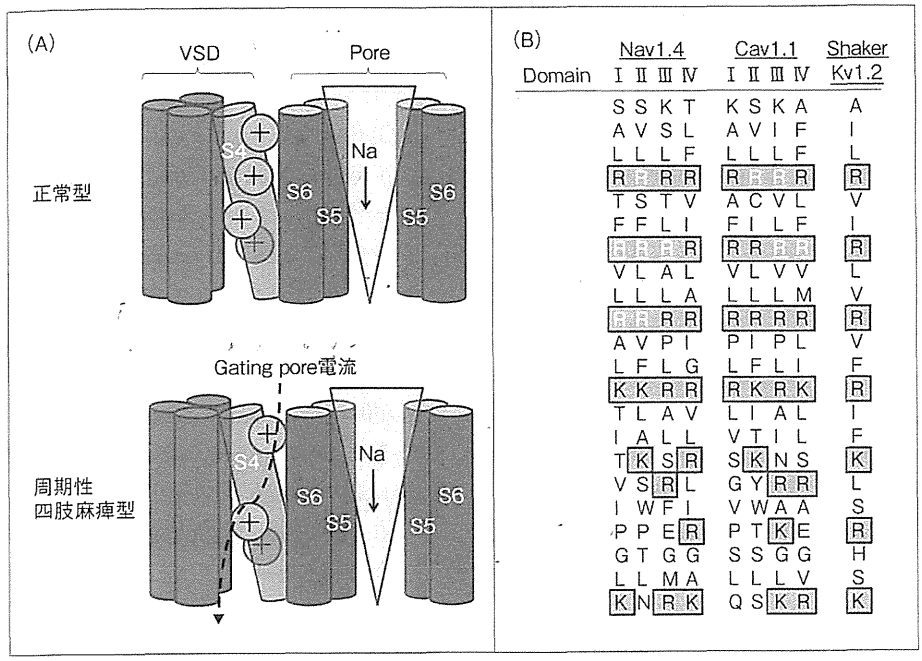

図 3　電位感受性ドメイン(VSD)とgating pore電流

A：Nav1.4の4つのドメインのうち，1つを中心に示す．Naイオンが通過するポアは他の3つのドメインのS5およびS6と組み合わさって構成される(上段：正常型)．S4に存在する正電荷に帯電したアミノ酸が変異することで，gating pore電流が生じる(下段：周期性四肢麻痺型)．

B：Nav1.4，Cav1.1，およびShaker/Kv1.2の各ドメインS4のアミノ酸配列を示す．規則正しく正電荷のアミノ酸が3アミノ酸ごとに並ぶのがわかる．一次性低K性周期性四肢麻痺の原因として報告されている変異部位を白抜き下線で示す．

tuans)から重症(myotonia permanens)までスペクトラムに幅がある．

PMC：寒冷により誘発される筋のこわばりを特徴とする．ときに弛緩性筋力低下や麻痺に至る．筋のこわばりは反復活動で増悪するパラミオトニーという特徴をもつ．力強く開閉眼を繰り返すと開眼できなくなる．

HyperPP：高K血症を伴う弛緩性麻痺発作が特徴である．呼吸不全は通常生じない．麻痺間欠期には，軽いミオトニーや，筋電図検査上でミオトニー放電が認められる．カリウム経口摂取，運動後の安静，寒冷は発作の誘因・増悪因子である．患者の変異チャネルでは遅い不活化の障害も併せもつものが多い[3]．

2. 麻痺症状を主症状とする筋チャネル病

① 低K性周期性四肢麻痺1型，2型 (hypokalemic periodic paralysis type 1, type 2：HypoPP1，HypoPP2)

低K血症を伴う弛緩性麻痺発作を特徴とする．本症の発作はHyperPPに比べて持続時間が長い．ミオトニーは認めず，ミオパチーや永続的な筋力低下を生じることがある．

HypoPP1は骨格筋型Caチャネル(Cav1.1)をコードする*CACNA1S*遺伝子の変異，HypoPP2は*SCN4A*の変異により生じる[2-4]．これらの共通点は，VSD中のS4にあるgating chargeが他のアミノ酸に変異している点である．2つの異なるチャネル異常が同一疾患の原因となる理由として，gating pore電流とよばれる，通常のポアとは別の経路による漏洩電流が生じることが示されている[5,6](図3；「サイドメモ1」参照)．現在まで報告されているHypoPP2例は，Nav1.4のDⅠ，D

Ⅱ，DⅢの gating charge の変異である．DⅣの gating charge の変異はPMCの表現型であることが知られており，HypoPP2の症例はない[2,7]．これはNav1.4における機能・構造上の差異によることが示唆されている．Nav1.4の個々のドメインは違う挙動を示すことが示されており，DⅢ，DⅡ，DⅠ，DⅣの順に活性化し，とくにDⅣのVSDの挙動は遅く，Nav1.4の速い不活化に関与することが示唆されている[8,9]．DⅣでは複数の gating charge に変異を導入してはじめて gating pore 電流が流れることが報告されており，DⅣのVSDにおけるhydrophobic plugの構成が他の3ドメインとは違うことが想像されている[8,10,11]．多くのHypoPP変異にみられる gating pore 電流は膜電位が過分極状態で活性化される性質をもち，その結果，安静時でも細胞内へ陽イオンが流れつづけることとなり，細胞膜の興奮性が上昇した状態となる．

Gating pore 電流については，アフリカツメガエルの卵母細胞を用いた cut-open 電位固定法によるNav1.4チャネルの解析を通して理解が深まった[5-7]．近年，HypoPP変異を導入したNav1.4トランスジェニックマウス[12]およびCav1.1トランスジェニックマウス[13]を用いた解析により，両者は gating pore 電流と考えられる病的な漏洩電流が原因で麻痺症状を呈することが示された．このことから，病的な漏洩電流を呈することがHypoPPに共通する病因と考えられる．

② 高K性周期性四肢麻痺(HyperPP)

前述のため略．

サイドメモ1

VSDのhydrophobic plugとgating pore電流
——Shaker Kチャネル

Gating pore 電流は，歴史的にはShaker Kチャネルにおいてはじめて示された[22]．S4の1つ目の gating charge であるR362をヒスチジンに置換すると，膜電位が過分極することでプロトン電流が流れることがわかった．これは電位感受性ドメイン内で細胞内外を隔てる領域が非常に狭い部分に集約されており，かつその狭い領域が電位を感受する電場“electric field”の集約している領域であることを示唆している．その後，この細胞内外を隔てる領域を構成するものとして，S1～S3に存在する疎水性アミノ酸残基の重要性がわかってきている[23,24]（下図）．これらのShaker Kチャネルの研究は，HypoPP2のNav1.4における gating pore 電流の発見につながっている．

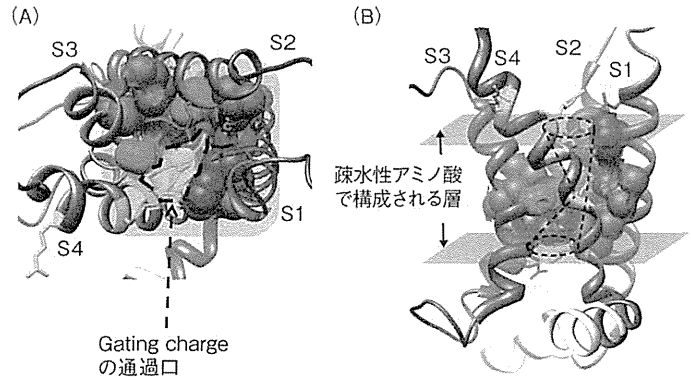

Kv1.2におけるhydrophobic plug/layer

Kv1.2の電位感受性ドメインの down state(安静時)を上からみた様子(A)，横からみた様子(B)．リボンで示しているのはKv1.2のS1～S4の backbone である．そのなかに含まれる疎水性アミノ酸を球体(フェニルアラニンを紫，その他を緑)で示し，その占拠部位を明らかにしている．S4に含まれる gating charge，およびS1，S2，S3に含まれる陰性電荷をもつアミノ酸はいずれも赤スティックで示している．こうしてみると疎水性アミノ酸で取り囲まれた狭い通路に gating charge(黄色)が並んでいることがわかる(破線内)．図はProtein Data Base ID3LUTをもとに作成．

③ 先天性筋無力症候群
(congenital myasthenic syndrome：CMS)

筋無力症，筋委縮，軽度の顔面奇形を特徴とする．多くは骨格筋アセチルコリンレセプター(AchR)の種々のサブユニットの変異などによる(「サイドメモ2」参照)．*SCN4A* 遺伝子変異による報告[14]があり，臨床病型の第4型に属する．

④ Andersen-Tawil症候群

周期性四肢麻痺，心室性不整脈やQT延長，奇形の三徴を特徴とするが，三徴がそろわない例も多い．10歳前後で，動悸や失神といった心症状か，麻痺発作で発症する．内向き整流性Kチャネル2.1(Kir2.1)をコードする *KCNJ2* 遺伝子の変異が原因で，常染色体優性遺伝である[4]．詳しくは本特集，木村「アンダーセン症候群」の稿に譲る．

サイドメモ2　先天性筋無力症候群(CMS)

神経筋接合部に発現する分子の遺伝子変異により生じ，現在までに，①AchRの各サブユニット，②ラプシン，③アグリン，④骨格筋特異的受容体チロシンキナーゼ(MuSK)，⑤Dok-7，⑥プレクチン，⑦グルタミン-フルクトース6リン酸アミノ基転移酵素，⑧コラーゲンQ(ColQ)，⑨β2ラミニン，⑩コリンアセチルトランスフェラーゼ，の遺伝子異常が同定されている[25]．これらに加えて，*SCN4A* 遺伝子変異による報告がある[14]．臨床型としては4病型に分類される．1型はAchR動態の異常によるもので，上記の①による．1型はさらに，イオンチャネルの開口時間が異常に延びるスローチャネル症候群と，イオンチャネルの開口時間が短縮するファーストチャネル症候群に大別される．スローチャネル症候群はCMSのなかで唯一のgain-of-functionによる優性遺伝性疾患で，成人発症の例も多くみられる．2型は終板AchR欠損症であり，重症筋無力症に似た病態で，①～⑦によるものが報告されている．3型は終板Achエステラーゼ(AchE)欠損症である．AchE分子はColQ分子と蛋白複合体を形成していることから，⑧により終板のAchEが欠損する．ColQ分子が組織特異的な発現をすることを利用したprotein-anchoring therapyの研究が進んでいる．4型は発作性無呼吸を伴う型で，上記⑩および *SCN4A* 遺伝子異常による例がこれにあたる．

3. 筋小胞体障害を主とする筋チャネル病

筋小胞体上に発現するイオンチャネル異常による筋チャネル病も知られている．具体的にはここで紹介する悪性高熱症，セントラルコア病といったリアノジンレセプター異常による疾患以外にも，Brody病など筋小胞体カルシウムATPase(SERCA)の異常による疾患などがある．

リアノジンレセプターは最大のイオンチャネルで，ホモテトラマーの構造をとる．小胞体/筋小胞体の膜上に位置し，細胞内カルシウム(Ca^{2+})濃度の維持に関与する．哺乳類にはRyR1～3までのアイソフォームをもち，とくに骨格筋に発現しているのはRyR1である[15]．RyR2はおもに心筋に発現し，カテコラミン感受性多形性心室頻拍(CPVT)などの発症に関連するが，詳しくは本特集，住友「カテコラミン誘発多形性心室頻拍(CPVT)とその亜型」の稿に譲る．ここではRyR1に関連する悪性高熱症とセントラルコア病を中心に述べる．このほか，*RYR1* 遺伝子変異は先天性ミオパチーであるマルチミニコア病やネマリンミオパチーとの関連も示唆されている．

① **悪性高熱症**……*RYR1* 遺伝子の変異により生じる致死性疾患である．体温の異常上昇，代謝性アシドーシス，低酸素症，頻脈，筋硬直を伴う横紋筋融解症を臨床的特徴とする．吸入麻酔薬，脱分極性筋弛緩薬，激しい運動や高温環境の曝露などが誘因で発症することが多い．誘因がなければ，*RYR1* 変異の保持者であっても発症しないことも多いため，正確な疾患頻度は不明である．本症の病態生理は変異RyR1の誘因因子に対する感受性が上昇しているため，筋小胞体から細胞内へのCa^{2+}漏洩が起こり，細胞内Ca^{2+}恒常性を維持できなくなるためと考えられている．発症後，速やかなダントリウムによる治療が重要である[12]．

② **セントラルコア病**……先天性ミオパチーのなかで最多頻度と考えられている．*RYR1* の変異により生じ，常染色体優性および劣性遺伝形式をもつが，同一家系のなかでも重症度にばらつきがみられる．臨床的特徴は筋委縮，精神発達の軽度の遅延に続く処女歩行の遅れ，側彎などの骨格系異常である．多くの患者が悪性高熱症を発症する

リスクをもつ．疾患名は筋病理所見で，ヒラメ筋などに代表される遅筋(Type 1線維)内に，ミトコンドリアと酸化酵素を欠いた“コア”とよばれる構造物がみられることによる．本症での変異RyR1の機能異常は，①筋小胞体から細胞内へのCa^{2+}漏洩と，②興奮収縮連関におけるCav1.1とRyR1との連関破綻とが示唆されている[15]．

二次性骨格筋チャネル病

1. 筋強直性ジストロフィー (dystrophia myotonica：DM)

成人の筋ジストロフィーのなかで最多である．筋萎縮・筋力低下，ミオトニーを主徴とする常染色体優性遺伝性疾患で，1型(DM1)と2型(DM2)が知られている．DM1は19番染色体上の*DMPK*遺伝子にあるCTG反復配列の反復回数延長(>50回)が原因であり，わが国ではほとんどがDM1である．DM1のおもな病態については，CTG反復配列伸長に起因したスプライシング因子の量的変化による種々のmRNAのスプライシング異常であることが明らかになりつつある．ミオトニーはスプライシング異常によりClC-1の発現が低下することで生じることが証明されている[16]．また，ClC-1以外の骨格筋イオンチャネルのスプライシング異常として，RyR1[17]，SERCA1型および2型[17]，Cav1.1[18]のスプライシング異常が同定され，筋委縮・筋力低下に関連する可能性が示唆されている．

2. 甲状腺中毒性周期性四肢麻痺 (thyrotoxic periodic paralysis：TPP)

甲状腺機能亢進症患者に起こる二次性筋チャネル病で，症状は一次性HypoPPに似る．アジアとラテンアメリカの男性に多い．近年，海外のTPP患者の33%に新規遺伝子*KCNJ18*の変異が同定された[19]．*KCNJ18*はKir2.6をコードしており，プロモーター領域に甲状腺ホルモン応答配列が存在することから，上昇した甲状腺ホルモンの作用でKir2.6の発現量が増加し，機能異常を有する変異Kir2.6の作用で骨格筋細胞膜の興奮性が上昇すると考えられている[19]．

一方，この*KCNJ18*変異のみつかった人種の内訳をみると，ブラジル・フランス・アメリカの30人のTPP中5人，香港の83人中1人，シンガポールの27人中7人と，TPPの多いとされる地域のなかでも差がみられる[19]．この点について近年，香港[20]およびタイ[21]からゲノムワイド関連解析(GWAS)の報告があいついでなされたが，いずれの報告でも*KCNJ18*については検出されなかった．この2報のGWASではともに，もっとも有力な疾患関連遺伝子座位として17番染色体長腕，*KCNJ2*遺伝子の下流に位置する領域が検出された．*KCNJ2*遺伝子と物理的に近い領域であることから，機能的関連も想像されているが，詳細は不明である．

今後の展望

筋チャネル病の診断は，臨床診断を進めていき，最終的には遺伝子解析による変異同定が確定診断となる．ただし，同一の変異症例・同一家系のなかでも症状の程度や，場合によっては表現型が違うことも経験される．新規変異の場合にはチャネル機能解析まで行い，変異チャネルの機能異常が症状を説明しうることを示すことが望まれる．これらの解析を通じてミオトニー症候群については理解が深まった．一方，麻痺を主症状とする疾患群についてはHypoPP1・HypoPP2におけるgating pore電流の研究により共通する病態生理の理解は深まっている．TPPは多くの原因遺伝子が存在する症候群と考えられ，不明な点も多く，より正確な臨床診断，患者群の集積が望まれる．遺伝情報解析のテクノロジーは，次世代シークエンサーの開発など，近年めざましい進歩がみられている．これらの技術を生かすためには臨床診断による，できるかぎり詳細で正確な疾患群の集積が必要である．また，Shakerチャネルにおける研究がHypoPPのgating pore電流へつながったように，結晶解析・構造解析を含むチャネル研究は今後もイオンチャネル病解明に向けて重要な役割を担うと考えられる．

文献

1) Matthews, E. et al.: *Brain*, **133**：9-22, 2010.
2) Cannon, S. C.: *J. Physiol.*, **588**：1887-1895, 2010.
3) Cannon, S. C.: *Ann. Rev. Neurosci.*, **29**：387-415, 2006.

4) Venance, S. L. et al.: *Brain*, **129**: 8-17, 2006.
5) Sokolov, S. et al.: *Nature*, **446**: 76-78, 2007.
6) Sokolov, S. et al.: *Proc. Natl. Acad. Sci. USA*, **105**: 19980-19985, 2008.
7) Francis, D. G. et al.: *Neurology*, **76**(19): 1635-1641, 2011.
8) Chanda, B. and Bezanilla, F.: *J. Gen. Physiol.*, **120**(5): 629-645, 2002.
9) Goldschen-Ohm, M. P. et al.: *Nat. Commun.*, **15**(4): 1350, 2013.
10) Capes, D. L. et al.: *Proc. Natl. Acad. Sci. USA*, **109**(7): 2648-2653, 2012.
11) Gosselin-Badaroudine, P. et al.: *Proc. Natl. Acad. Sci. USA*, **109**(47): 19250-19255, 2012.
12) Wu, F. et al.: *J. Clin. Invest.*, **121**(10): 4082-4094, 2011.
13) Wu, F. et al.: *J. Clin. Invest.*, **122**(12): 4580-4591, 2012.
14) Tsujino, A. et al.: *Proc. Natl. Acad. Sci. USA*, **100**: 7377-7382, 2003.
15) Lanner, J. T.: *Adv. Exp. Med. Biol.*, **740**: 217-234, 2012.
16) Mankodi, A. et al.: *Mol. Cell*, **10**: 35-44, 2002.
17) Kimura, T. et al.: *Hum. Mol. Genet.*, **14**(15): 2189-2200, 2005.
18) Tang, Z. Z. et al.: *Hum. Mol. Genet.*, **21**(6): 1312-1324, 2012.
19) Ryan, D. P. et al.: *Cell*, **140**: 88-98, 2010.
20) Cheung, C. L. et al.: *Nat. Genet.*, **44**(9): 1026-1029, 2012.
21) Jongjaroenprasert, W. et al.: *J. Hum. Genet.*, **57**(5): 301-304, 2012.
22) Starace, D. M. and Bezanilla, F.: *Nature*, **427**(6974): 548-553, 2004.
23) Campos, F. V. et al.: *Proc. Natl. Acad. Sci. USA*, **104**(19): 7904-7909, 2007.
24) Chen, X. et al.: *Proc. Natl. Acad. Sci. USA*, **107**(25): 11352-11357, 2010.
25) 大野欽司：臨床神経，**52**：1159-1161，2012.

*　　*　　*

Pediatric Neurology xxx (2015) 1–5

Contents lists available at ScienceDirect

Pediatric Neurology

journal homepage: www.elsevier.com/locate/pnu

Original Article

Phenotypic Variability in Childhood of Skeletal Muscle Sodium Channelopathies

Harumi Yoshinaga MD [a,*], Shunichi Sakoda MD [b], Takashi Shibata MD [a], Tomoyuki Akiyama MD [a], Makio Oka MD [a], Jun-Hui Yuan MD, PhD [b], Hiroshi Takashima MD, PhD [b], Masanori P. Takahashi MD [c], Tetsuro Kitamura MD [d], Nagako Murakami MD [d], Katsuhiro Kobayashi MD [a]

[a] *Department of Child Neurology, Okayama University Graduate School of Medicine, Dentistry and Pharmaceutical Sciences, Okayama, Japan*
[b] *Department of Neurology and Geriatrics, Kagoshima University Graduate School of Medical and Dental Sciences, Medical School, Kagoshima, Japan*
[c] *Department of Neurology, Osaka University Graduate School of Medicine, Osaka, Japan*
[d] *Department of Pediatrics, Nipponkokan Fukuyama Hospital, Hiroshima, Japan*

ABSTRACT

BACKGROUND: Mutations of the *SCN4A* gene cause several skeletal muscle channelopathies and overlapping forms of these disorders. However, the variability of the clinical presentation in childhood is confusing and not fully understood among pediatric neurologists. **PATIENTS:** We found three different mutations (p.V445M, p.I693L, and a novel mutation, p.V1149L) in *SCN4A* but not in the *CLCN1* gene. The patient with p.V445M showed the clinical phenotype of sodium channel myotonia, but her clear symptoms did appear until 11 years of age. Her younger sister and mother, who have the same mutation, displayed marked intrafamilial phenotypic heterogeneity from mild to severe painful myotonia with persistent weakness. The patient with p.I693L exhibited various symptoms that evolved with age, including apneic episodes, tonic muscular contractions during sleep, fluctuating severe episodic myotonia, and finally episodic paralyses. The patient with the novel p.V1149L mutation exhibited episodic paralyses starting at 3 years of age, and myotonic discharges were detected at 11 years of age for the first time. **CONCLUSION:** The present cohort reveals the complexity, variability, and overlapping nature of the clinical features of skeletal muscle sodium channelopathies. These are basically treatable disorders, so it is essential to consider genetic testing before the full development of a patient's condition.

Keywords: sodium channelopathy, *SCN4A*, mutation, myotonia, periodic paralysis, electromyography, genetic testing

Pediatr Neurol 2015; ■: 1-5

Introduction

Mutations of the *SCN4A* gene, which encodes the skeletal muscle voltage-gated sodium channel $Na_v1.4$, cause various skeletal muscle disorders. Paramyotonia congenita, sodium channel myotonia (SCM), hyperkalemic periodic paralysis (hyperPP), and hypokalemic periodic paralysis are representatives of these disorders. To date, more than 60 mutations of *SCN4A* have been reported.[1,2] However, these disorders are not described adequately in the field of pediatric neurology because of phenotypic heterogeneity[3] and the complicated pathophysiology of ion channels.[1,2] Recently, electrophysiological protocols for the diagnosis of muscle channelopathies have became prevalent and prompted the application of genetic testing.[4,5]

Over the past decade, we experienced five patients with three underlying genetic bases for their skeletal muscle sodium channelopathies. They exhibited various phenotypes because of the different heterozygous point mutations. The diagnostic process for each patient was difficult

Article History:
Received November 10, 2014; Accepted in final form January 22, 2015

* Communications should be addressed to: Dr. Yoshinaga; Department of Child Neurology; Okayama University Graduate School of Medicine; Dentistry and Pharmaceutical Sciences; Shikatacho 2-5-1; Okayama, 700-8558, Japan.
E-mail address: magenta@md.okayama-u.ac.jp

0887-8994/$ – see front matter © 2015 Elsevier Inc. All rights reserved.
http://dx.doi.org/10.1016/j.pediatrneurol.2015.01.014

because of the phenotypic variability in childhood. These patients provide some clues that will yield a better understanding and diagnosis of skeletal muscle sodium channelopathies.

Methods

DNA analysis

We analyzed the nucleotide sequences of *SCN4A* and the skeletal muscle chloride channel *CLCN1* genes of the patients and their parents with the Sanger method. A *CLCN1* mutation causes myotonia congenita, the phenotype that is often similar to SCM. Written informed consent was obtained from the parents for the mutation screening. This study was approved by the ethics committee of Kagoshima University Graduate School of Medical and Dental Sciences.

Electrophysiological analysis

We performed needle electromyography to check for myotonic discharges. Then we analyzed the compound muscle action potential (CMAP) amplitude in response to a short (10-12 seconds) exercise test with/without muscle cooling and a long (5-minute) exercise test, following the protocols proposed by Fournier et al.[4,5]

Patient descriptions

Clinical and electrophysiological features of all patients are summarized in Table 1.

Patient I-1

The proband was a 13-year-old girl who visited us in 2011 with myotonic symptoms. She was delivered by cesarean section and showed intellectual disability with speech delay at 1 year of age. By 3 years of age, she had developed walking difficulties and was diagnosed with paroxysmal kinesigenic choreoathetosis. Carbamazepine failed to relieve her symptoms. She developed grip and eyelid myotonia at 11 years of age. Then, molecular genetic analysis revealed no expansion of the repeat length at the *DM1* locus. Her symptoms were induced by exercise, but she never showed paradoxical myotonia. Her leg stiffness occurred during the initial 20 m of a 100-m run. At 12 years of age, she experienced a respiratory problem following a difficult extubation after surgery with general anesthesia and was referred to us for further examination. She was short in height, with a short neck and scoliosis. Her IQ was 57. Percussion of her tongue and palms easily elicited her myotonia. She exhibited dysarthria because of her myotonia. Her myotonia occurred not only immediately after movement initiation, but also with a delayed onset after a brief rest following long exercise. Her myotonia showed warm-up phenomenon and cold insensitivity. Cold temperature was a precipitating factor for her myotonia, along with fatigue, lack of sleep, and emotional stress. Her muscle consistency was increased, and her extremities and buttocks were hypertrophic. Serum creatine kinase and electrolytes were normal. Needle electromyography revealed myotonic discharges. CMAP amplitude did not change during short and long exercise tests. DNA sequencing revealed a c.1333G>A (p.V445M) mutation in *SCN4A* but not in the *CLCN1* gene. Her younger sister (patient I-2) and her mother (patient I-3) also showed myotonia, the severity of which was remarkably different. An identical mutation was found in both the mother and sister. All three patients in this family were diagnosed with SCM.

Patient I-2

This is the younger sister of the proband. This patient has autism, and her myotonia was the mildest of the three

TABLE 1.
Clinical and Electrophysiological Features of the Five Patients

Patient	I-1	I-2	I-3	II	III
SCN4A mutation	p.V445 M	p.V445 M	p.V445 M	p.I693 L	p.V1149 L
Diagnosis	SCM	SCM	SCM	SCM with PP	HyperPP with myotonia
Gender	F	F	F	M	M
Age at onset	3 years	2 years	3 years	7 days	3 years
Age at diagnosis	14 years	12 years	41 years	7 years	12 years
Clinical myotonia	+	+	+	+	-
Severity	Moderate	Mild	Severe	Mild to severe, fluctuating	/
Warm-up	+	-	+	-	/
Paradoxical myotonia	-	-	-	-	/
Cold sensitivity	-	-	-	-	/
Delayed myotonia	+	-	+	-	/
Painful myotonia	-	-	+	+	/
Episodic weakness	-	-	-	+	+
Persistent weakness	-	-	+	+	-
Muscle hypertrophy	+	-	+	+	-
Muscle atrophy	-	-	+	+	-
Potassium sensitivity	/	/	/	/	-
Myotonic discharge	+	/	/	+	+
Short exercise test	No change	/	/	No change	No change
Long exercise test	No change	/	/	No change	Initial increase Delayed decrease
Fournier pattern I-V	III	/	/	III	Unclassified

Abbreviations:
HyperPP = Hyperkalemic periodic paralysis
PP = Periodic paralysis
SCM = Sodium channel myotonia

affected family members and she sometimes would go full days without any myotonia. Electrophysiological analysis was impossible because of her intellectual disability. Myotonia occurred just after initiation of movement, and dysarthria was only observed upon speech initiation. Myotonia could be induced by percussion of tongue and thumbs. Cold and sleep deprivation were precipitating factors. Mexiletine was partially effective for her myotonia.

Patient I-3

This is the mother of proband. She suffered from severe myotonia with pain and was the most severe case in her family. External ocular muscles and swallowing muscles were involved. During her pregnancies, she used a wheelchair because of exacerbation of myotonia. She gradually developed muscle atrophy in her distal extremities. Severe pain was reported in the left hand and right soleus. Manual muscle testing revealed weakness in all tested muscles. Various drugs, including mexiletine, acetazolamide, and phenytoin, failed to ameliorate her symptoms.

Patient II

This patient is a 13-year-old boy harboring the SCN4A mutation c.2077A>C (p.I693L) and who we reported on in 2012.[6] At 7 days after birth, he experienced apneic episodes with generalized muscle stiffness while crying. He often exhibited tonic muscle contraction of the extremities during sleep starting at 11 months of age. At 2 years of age, severe episodic myotonia with daily fluctuation began. After age 7, he started to suffer from paralytic episodes several times a year. Episodic weakness lasted from hours to several days with loss of muscle consistency in both thighs. He also had several physical characteristics resembling Schwartz-Jampel syndrome.[7] But causative *HSPG2* gene analysis and immunohistochemical staining of perlecan in biopsied muscle, which is encoded by *HSPG2*, were normal. Functional analyses of p.I693L mutated Nav1.4 heterologously expressed in vitro revealed enhanced activation and disruption of slow inactivation, which were consistent with an overlapping form of SCM and periodic paralysis. Acetazolamide, mexiletine, and phenytoin had some beneficial effects on his severe episodic myotonia.

Patient III

This 14-year-old boy was age 9 when he was referred to us for paralytic episodes. His mother had had two episodes of sudden paralysis of the extremities accompanied by elevated serum creatine kinase during her pregnancies. His perinatal and developmental history was normal. At 3 years of age, paralysis of extremities suddenly appeared on the morning of the day following a febrile episode. Then, elevated serum creatine kinase and normal potassium levels suggested normokalemic periodic paralysis. His paralytic episode resolved within a week without residual muscle weakness. At age 9, he suffered from sudden, painful muscle paralysis of the extremities after a soccer game. His creatine kinase level was transiently elevated to 3685 U/L. At a later date, physical and neurologic examinations, including electrophysiological tests, glucose plus insulin or potassium loading tests, were all normal. At age 11, reexamination via needle electromyography revealed weak myotonic discharges. Therefore, we retried all the examinations. The short exercise test revealed no change in CMAP amplitude. However, during the long exercise test, an early increase (22.7%) and delayed decrease in CMAP amplitude after 5 minutes of isometric exercise were observed. DNA sequence analysis revealed a novel heterozygous mutation of c.3445G>T (p.V1149L) in *SCN4A*. This mutation was also detected in his mother. His final diagnosis was hyperPP with myotonia. His paralytic symptoms disappeared completely upon administration of carbamazepine.

Discussion

Myotonia is the cardinal symptom in paramyotonia congenita, SCM, and the overlapping forms of paramyotonia congenita and hyperPP (paramyotonia congenita/hyperPP).[8] But myotonia is weak or absent in hyperPP and essentially absent in hypokalemic periodic paralysis.[7] The overlapping forms of sodium channelopathies are not unheard of, whereas paramyotonia congenita/hyperPP is relatively common.[9,10] As for normokalemic periodic paralysis, which was suggested in patient III at disease onset, it has been argued that normokalemic periodic paralysis is identical to hyperPP, because the underlying mutations of normokalemic periodic paralysis are the same as for hyperPP.[7,11] Moreover, hypotonia, stridor, and laryngospasm among neonates were found to be the symptoms of sodium channelopathies by genetic testing.[12-14] Skeletal muscle sodium channelopathies are basically treatable disorders, but can be fatal, as in patient II, who experienced a life-threatening episode at 7 days after birth. Thus, early diagnosis is essential to ensure good outcomes of affected neonates. Clinical and electrophysiological characteristics of skeletal muscle sodium and chloride channel myotonia are summarized in Table 2.[1,2,8-10,15]

In our experience, the difficulty in clinical diagnosis of skeletal muscle sodium channelopathy lies in the phenotypic variability during a patient's development. It took quite some time to arrive at a definitive diagnosis in patients I-1 and III because clear symptoms did not appear until 11 years of age. The grip and eyelid myotonias of patient I-1 appeared at 11 years of age, which easily suggested myotonic disorders. The subclinical myotonia of patient III was suddenly detected as myotonic discharges at age 11, which strongly suggested hyperPP.[7] Patient II was an uncommon case with resemblance to Schwartz-Jampel syndrome. We originally excluded Schwartz-Jampel syndrome by immunohistochemical and genetic analyses; thereafter, the exploration of pathogenesis was directed to sodium channel myotonias.

We would like to refer to usefulness of the electrophysiological protocols published by Fournier et al.[4,5] They investigated the relationship between electromyographic findings and specific channel protein mutations and identified five different electromyographic patterns that correspond to the subgroups of mutations and clinical categories of muscle channelopathy.

Electrophysiological analysis was performed on patients I-1, II, and III, and all patients showed myotonic discharges. Flat patterns of CMAP amplitude in both short and long

TABLE 2.
Clinical and Electrophysiological Characteristics of Skeletal Muscle Sodium and Chloride Channel Myotonias

Disorder	RMC	DMC	SCM	PMC	HyperPP/PMC	HyperPP
Gene mutation	CLCN1	CLCN1	SCN4A	SCN4A	SCN4A	SCN4A
Age at onset (years)	<10, late	<10, early	<10	<10, early	<10	<10
Clinical myotonia	+	+	+	+	+	+/-
Severity	Moderate to severe	Mild to moderate	Mild to severe	Mild to moderate	Mild to severe	Mild
Warm up	+	+	+/-	-	-	+
Paradoxical myotonia	-	-	-	+	+	+/-
Cold sensitivity	+/-	+/-	+/-	+	+	+/-
Delayed myotonia	-	-	+/-	-	-	-
Painful myotonia	+/-	-	+/-	-	-	-
Episodic weakness	+/-	-	-	+	+	+
Persistent weakness	+/-	-	-	-	+/-	+/-
Muscle hypertrophy	+	+/-	+/-	+/-	+/-	-
Muscle atrophy	+/-	+/-	-	-	-	-
Potassium sensitivity	-	-	+	+/-	+	+
Myotonic discharge	+	+	+	+	+	+/-
Short exercise test	Initial decrease	No change or initial decrease	No change	Decrease	Increase*	Increase
Long exercise test	No change or initial decrease	No change or initial decrease	No change	Decrease	Changes similar to PMC or SCM or hyperPP†	Initial increase Delayed decrease
Fournier pattern I-V	II	II/III	III	I	/	IV

Abbreviations:
DMC = Dominant myotonia congenita (Thomsen disease)
HyperPP = Hyperkalemic periodic paralysis
HyperPP/PMC = Overlapping form of hyperkalemic periodic paralysis and paramyotonia congenita
PMC = Paramyotonia congenita
RMC = Recessive myotonia congenita (Becker disease)
SCM = Sodium channel myotonia
* Data from reference 14.
† Data from reference 15.

exercise tests were observed in patients I-1 and II, which corresponded to Fournier pattern III and suggested SCM for both patients. Although patient III was not classified into any Fournier patterns because of the conflict of the flat pattern in the short exercise test and the initial increase and delayed decrease pattern in the long exercise test. However, SCM or hyperPP was suggested for this patient. In addition to delayed myotonia, patient I-1 had myotonia immediately after movement initiation, which showed warm-up phenomenon and cold insensitivity. This type of myotonia is usually observed after rest in chloride channel myotonia (i.e., myotonia congenita caused by *CLCN1*). For this reason, *CLCN1* should be considered another candidate gene for mutation analysis in such a case. Nevertheless, this electrophysiological analysis can only be performed on children who are willing to be cooperative during the examination.

We also illustrated the location of the mutations associated with skeletal muscle sodium channelopathies and the three mutations of our patients on a schematic diagram of the α-subunit of $Na_v1.4$ (Figure).[1,2] From this diagram, it is clear that mutations are abundant at the inner side of the sarcoplasmic membrane, and several hotspots were observed that corresponded to the disorders.

In a previous report,[16] the patients with p.V445M exhibited severe painful myotonias, especially in the chest. The region of pain was different from that in the present cohort: patient I-3 had pain in the extremities, whereas the myotonias of patient I-1 and I-2 were painless. Patient I-3's muscle atrophy and persistent weakness are signs that are rarely observed in SCM. It is unclear whether her muscle weakness resulted from severe myotonia or age-dependent myopathy. However, the family of patient I exhibited significant intrafamilial phenotypic heterogeneity and provided a key to understand the complexity of sodium channelopathy.

Concerning p.I693L of patient II, another substitution at the same site (p.I693T) has already been reported and could

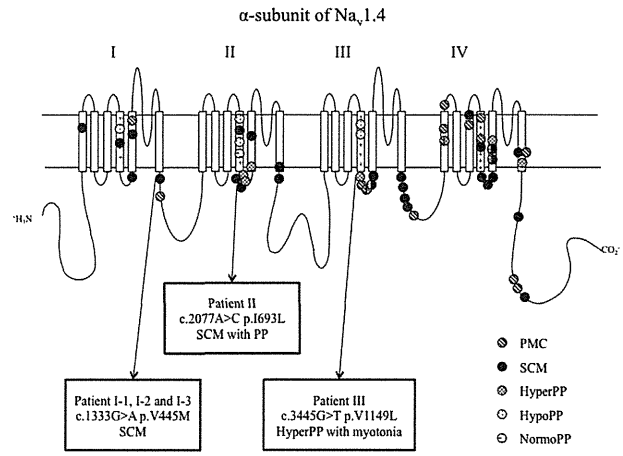

FIGURE.
Schematic representation of the α-subunit of $Na_v1.4$ showing the location of the mutations associated with paramyotonia congenita, sodium channel myotonia, hyperkalemic periodic paralysis, hypokalemic periodic paralysis, and normokalemic periodic paralysis[1,2] in addition to p.V445M, p.I693L, and p.V1149L of our patients. HyperPP = hyperkalemic periodic paralysis; hypoPP = hypokalemic periodic paralysis; normoPP = normokalemic periodic paralysis; PMC = paramyotonia congenita; PP = periodic paralysisSCM = sodium channel myotonia.

generate various phenotypes, including cold-induced weakness without stiffness,[17] muscle stiffness and episodic weakness,[4] neonatal hypotonia,[12] paramyotonia congenita,[18] and hyperPP.[11] Patient II was diagnosed with SCM with periodic paralysis.

Although p.V1149L in patient III was a novel mutation, it was located in a highly conserved mutation hotspot region. This mutation was absent in the Single Nucleotide Polymorphism database or 1000 Genomes Project database and was not found in 200 control DNA samples. Moreover, it was predicted to be possibly damaging and deleterious in PolyPhen2 and SIFT, respectively. In addition, this patient's mother, who harbors the same mutation, also experienced prolonged paralytic attacks twice during her pregnancies. Taken together, this mutation was considered to be causative in this family.

Herein, we have highlighted the complexity, variability, and overlapping nature of the clinical features of several skeletal muscle sodium channelopathies. A definite diagnosis is necessary for physicians to alleviate symptoms or even to save lives. A genetic study based on careful clinical examination and accurate electromyography tests is recommended. Special attention should also be paid to the evolution of clinical phenotypes. We hope our experiences will help pediatric neurologists better understand this group of disorders.

This study was supported in part by an Intramural Research Grant on the Nervous and Mental Disorders of NCNP and a Research Grant for Intractable Disease and the Research Committee for Applying Health and Technology of the Ministry of Health, Welfare and Labor of Japan.

References

1. Matthews E, Fialho D, Tan SV, et al. The non-dystrophic myotonias: molecular pathogenesis, diagnosis and treatment. *Brain*. 2010;133:9-22.
2. Simkin D, Bendahhou S. Skeletal muscle Na^+ channel disorders. *Front Pharmacol*. 2011;2:63.
3. Saleem R, Setty G, Khan A, Farrell D, Hussain N. Phenotypic heterogeneity in skeletal muscle sodium channelopathies: A case report and literature review. *J Pediatr Neurosci*. 2013;8:138-140.
4. Fournier E, Arzel M, Sternberg D, et al. Electromyography guides toward subgroups of mutations in muscle channelopathies. *Ann Neurol*. 2004;56:650-661.
5. Fournier E, Viala K, Gervais H, et al. Cold extends electromyography distinction between ion channel mutations causing myotonia. *Ann Neurol*. 2006;60:356-365.
6. Yoshinaga H, Sakoda S, Good JM, et al. A novel mutation in SCN4A causes severe myotonia and school-age-onset paralytic episodes. *J Neurol Sci*. 2012;315:15-19.
7. Lehmann-Horn F, Rüdel R, Jurkat-Rott K. Nondystrophic myotonias and periodic paralyses. In: Engel AG, Franzini-Armstrong C, eds. *Myology*. 3rd ed. New York: McGraw-Hill; 2004:1257-1300.
8. Heatwole CR, Moxley 3rd RT. The nondystrophic myotonias. *Neurotherapeutics*. 2007;4:238-251.
9. Kim J, Hahn Y, Sohn EH, et al. Phenotypic variation of a Thr704Met mutation in skeletal sodium channel gene in a family with paralysis periodica paramyotonica. *J Neurol Neurosurg Psychiatry*. 2001;70:618-623.
10. Hsu WC, Huang YC, Wang CW, Hsueh CH, Lai LP, Yeh JH. Paralysis periodica paramyotonica caused by SCN4A Arg1448Cys mutation. *J Formos Med Assoc*. 2006;105:503-507.
11. Song YW, Kim SJ, Heo TH, Kim MH, Kim JB. Normokalemic periodic paralysis is not a distinct disease. *Muscle Nerve*. 2012;46:914-916.
12. Matthews E, Guet A, Mayer M, et al. Neonatal hypotonia can be a sodium channelopathy: recognition of a new phenotype. *Neurology*. 2008;71:1740-1742.
13. Matthews E, Manzur AY, Sud R, Muntoni F, Hanna MG. Stridor as a neonatal presentation of skeletal muscle sodium channelopathy. *Arch Neurol*. 2011;68:127-129.
14. Lion-Francois L, Mignot C, Vicart S, et al. Severe neonatal episodic laryngospasm due to de novo SCN4A mutations: a new treatable disorder. *Neurology*. 2010;75:641-645.
15. Mankodi A. Myotonic disorders. *Neurol India*. 2008;56:298-304.
16. Rosenfeld J, Sloan-Brown K, George Jr AL. A novel muscle sodium channel mutation causes painful congenital myotonia. *Ann Neurol*. 1997;42:811-814.
17. Plassart E, Eymard B, Maurs L, et al. Paramyotonia congenita: genotype to phenotype correlations in two families and report of a new mutation in the sodium channel gene. *J Neurol Sci*. 1996;142:126-133.
18. Lee SC, Kim HS, Park YE, Choi YC, Park KH, Kim DS. Clinical Diversity of SCN4A-Mutation-Associated Skeletal Muscle Sodium Channelopathy. *J Clin Neurol*. 2009;5:186-191.

Stem Cell Research (2014) 12, 492–505

Available online at www.sciencedirect.com

ScienceDirect

www.elsevier.com/locate/scr

Perlecan is required for FGF-2 signaling in the neural stem cell niche☆

Aurelien Kerever[a], Frederic Mercier[b], Risa Nonaka[a], Susana de Vega[a], Yuka Oda[a], Bernard Zalc[c,d,e], Yohei Okada[f], Nobutaka Hattori[g], Yoshihiko Yamada[h], Eri Arikawa-Hirasawa[a,g,*]

[a] *Research Institute for Diseases of Old Age, Juntendo University Graduate School of Medicine, Tokyo, Japan*
[b] *Department of Tropical Medicine and Infectious Diseases, John A. Burns School of Medicine, University of Hawaii, Honolulu, HI, USA*
[c] *Université Pierre et Marie Curie-Paris 6, Centre de Recherche de l'Institut du Cerveau et de la Moelle Épinière (CRICM), UMRS 975, Paris, 75013 France*
[d] *Inserm, U 975, Paris, 75013 France*
[e] *CNRS, UMR 7225, Paris, 75013 France*
[f] *Department of Physiology and Kanrinmaru project, Keio University, School of Medicine, Shinjuku-ku, Tokyo, Japan*
[g] *Department of Neurology, Juntendo University School of Medicine, Tokyo, Japan*
[h] *National Institute of Dental and Craniofacial Research, NIH, Bethesda, MD, USA*

Received 10 September 2013; received in revised form 26 November 2013; accepted 21 December 2013
Available online 28 December 2013

Abstract In the adult subventricular zone (neurogenic niche), neural stem cells double-positive for two markers of subsets of neural stem cells in the adult central nervous system, glial fibrillary acidic protein and CD133, lie in proximity to fractones and to blood vessel basement membranes, which contain the heparan sulfate proteoglycan perlecan. Here, we demonstrate that perlecan deficiency reduces the number of both GFAP/CD133-positive neural stem cells in the subventricular zone and new neurons integrating into the olfactory bulb. We also show that FGF-2 treatment induces the expression of cyclin D2 through the activation of the Akt and Erk1/2 pathways and promotes neurosphere formation in vitro. However, in the absence of perlecan, FGF-2 fails to promote neurosphere formation. These results suggest that perlecan is a component of the neurogenic niche that regulates FGF-2 signaling and acts by promoting neural stem cell self-renewal and neurogenesis.

* Corresponding author at: Juntendo University Graduate School of Medicine, Research Institute for Diseases of Old Age, Building 10, Room 606, 2-1-1 Hongo, Bunkyo-ku, Tokyo 113–8421, Japan. Fax: +81 3 3814 3016.
E-mail address: ehirasaw@juntendo.ac.jp (E. Arikawa-Hirasawa).

1873-5061/$ - see front matter © 2013 The Authors. Published by Elsevier B.V. All rights reserved.
http://dx.doi.org/10.1016/j.scr.2013.12.009

Introduction

In the adult mouse brain, neurogenesis occurs continuously in at least two regions: the subventricular zone (SVZ) of the lateral ventricle (Altman, 1963, 1969; Doetsch et al., 1997) and the subgranular zone of the hippocampal dentate gyrus (Seki and Arai, 1993; Eriksson et al., 1998). In the adult SVZ, subsets of glial fibrillary acidic protein positive ($GFAP^+$) cells (type B cells) function as quiescent neural stem cells (Doetsch et al., 1999), although a portion of these cells are slowly dividing at any given time. These quiescent cells qualify as being activated when they begin to co-express the epidermal growth factor receptor (EGF-R) and come into contact with the ventricle (Pastrana et al., 2009). Then, they give rise to rapidly proliferating cells called "transit-amplifying cells" (type C cells), which stop expressing GFAP but still express EGF-R. The cells then differentiate into doublecortin (DCX)-expressing neuroblasts (type A cells) that migrate along the rostral migratory stream (RMS) towards the olfactory bulb (Lois and Alvarez-Buylla, 1994; Petreanu and Alvarez-Buylla, 2002). They finally integrate into both the granule cell layer (GCL) and glomerular layer (GL) of the olfactory bulb, where they express mature neuronal markers, such as NeuN (Winner et al., 2002).

The early signaling cues promoting the proliferation and differentiation of the neural stem and progenitor cells (NSPCs) are yet to be elucidated. Recent studies have proposed that blood vessels are critical elements of the neurogenic niches in both the hippocampus (Palmer et al., 2000) and the SVZ (Mercier et al., 2002; Shen et al., 2008; Tavazoie et al., 2008). In addition, Mercier et al. (2002) previously characterized basal lamina-like structures, termed fractones, in the vicinity of NSPCs in the adult SVZ. Fractones present extracellular branched fractal structures in direct contact with NSPCs in the adult neurogenic niche, thereby suggesting fractones' role in neurogenesis (Altman, 1963, 1969; Doetsch et al., 1997; Mercier et al., 2002, 2003).

Fractones are composed of different extracellular matrix (ECM) molecules, such as laminin (β1 and γ1 but not α1), collagen IV, nidogen, and perlecan (Mercier et al., 2002; Kerever et al., 2007). They are able to capture/bind the neurogenic growth factor FGF-2 from the extracellular environment. This trapping of FGF-2 involves binding to heparan sulfate chains (Kerever et al., 2007; Douet et al., 2012). Furthermore, FGF-2 promotes neurogenesis in developing (Raballo et al., 2000; Maric et al., 2007; Pastrana et al., 2009) and adult brains (Lois and Alvarez-Buylla, 1994; Palmer et al., 1995; Petreanu and Alvarez-Buylla, 2002).

We previously showed that perlecan (*HSPG2*), a major heparan sulfate proteoglycan (HSPG) in basement membranes, is present in both blood vessel walls and fractones in the neurogenic niche (Kerever et al., 2007). Perlecan interacts with extracellular molecules, growth factors, and cell surface receptors (Rapraeger, 1995; Winner et al., 2002; Chan et al., 2009), and is implicated in many biological functions in tissue development, homeostasis, and diseases (Arikawa-Hirasawa et al., 1995, 1999; Palmer et al., 2000; Arikawa-Hirasawa et al., 2001, 2002a, 2002b; Xu et al., 2010). Perlecan promotes growth factor receptor binding, such as FGF-2, to stimulate mitogenesis and angiogenesis (Yayon et al., 1991; Aviezer et al., 1994; Mercier et al., 2002; Shen et al., 2008; Tavazoie et al., 2008). A perlecan analog in Drosophila has also been implicated in the reactivation of proliferation in quiescent neural stem cells (NSCs) (Voigt et al., 2002).

Perlecan deficiency causes perinatal lethal chondrodysplasia in mice and in humans (Arikawa-Hirasawa et al., 1999; Costell et al., 1999; Arikawa-Hirasawa et al., 2001), and perlecan knockout ($HSPG2^{-/-}$) mice present impaired indian hedgehog expression and FGF-1 signaling and abnormal cephalic development (Arikawa-Hirasawa et al., 1999). $HSPG2^{-/-}$ mice die at or just before birth due to defects in tracheal cartilage. Furthermore, Giros and colleagues reported a disrupted distribution of sonic hedgehog (Shh) and impaired forebrain development in perlecan-null mice (Girós et al., 2007). We previously created perinatal lethality rescued ($Hspg2^{-/-}$-Tg) mice by expressing recombinant perlecan specifically in the cartilage of the perlecan-null ($HSPG2^{-/-}$) genetic background, in order to study the role of perlecan in tissue homeostasis in adult mice. We used these $HSPG2^{-/-}$-Tg mice to show that perlecan is critical for maintaining fast muscle mass and fiber composition, through regulation of myostatin signaling (Xu et al., 2010).

In the present report, we studied the role of perlecan in the maintenance and fate of NSCs, and in response to FGF-2 stimulation in the SVZ of $Hspg2^{-/-}$-Tg mice. The absence of perlecan resulted in the depletion of $CD133^+$ NSCs. In addition, FGF-2 treatment failed to induce an increase in activation of Akt and Erk1/2 pathways both *in vivo* and *in vitro* in the absence of perlecan. Furthermore, FGF-2 failed to induce cyclin D2 expression and to promote the formation of neurospheres. Taken together, our results indicate that the absence of perlecan is detrimental for $CD133^+$ NSC population and for adult neurogenesis, suggesting that it is a critical component of the adult neurogenic niche.

Materials and methods

Animals

Perlecan-null ($Hspg2^{-/-}$) mice die at birth because of premature cartilage development (Arikawa-Hirasawa et al., 1999). To restore cartilage abnormalities, we used a cartilage-specific Col2a1 promoter/enhancer to generate a perlecan transgenic mouse line (WT-Tg, $Hspg2^{+/+}$; Col2a1-Hspg2Tg/-), which expressed recombinant perlecan in cartilage (Tsumaki et al., 1999). We subsequently created lethality-rescued mice ($Hspg2^{-/-}$-Tg, $Hspg2^{-/-}$; Col2a1-Hspg2Tg/-) by mating the transgenic mice with heterozygous $Hspg2^{+/-}$ mice (Xu et al., 2010). We maintained these mice on the mixed genetic background of C57BL/6 and 129SvJ. In this study, WT-Tg mice (control) and $Hspg2^{-/-}$-Tg (perlecan knockout) mice were used. All animal protocols were approved by the Animal Care and Use Committee of Juntendo University.

BrdU incorporation and FGF-2 treatment assays

Mice that were 8–12 weeks old were used in this study. Nine-week-old mice were sacrificed 48 h after intracerebroventricular (ICV) injection of BrdU (1 μl of 40 mg/ml; WT-Tg, $n = 5$; $Hspg2^{-/-}$-Tg, $n = 5$). Eight-week-old mice received daily intraperitoneal injections of BrdU (50 mg/kg

of body weight) for 5 days. They were sacrificed 4 weeks after the fifth and last injections (WT-Tg, $n = 5$; Hspg2$^{-/-}$-Tg, $n = 5$). For FGF-2 stimulation in NSCs, 9-week-old mice were injected ICV with FGF-2 (1 μl, 0.075 μg/μl). Mice were sacrificed 48 h after ICV injections.

Histology

Mice were deeply anesthetized and perfused transcardially with cold paraformaldehyde (4%) in a 100 mM phosphate buffer, pH 7.4. Brains were dissected, immersed overnight in fixative, and transferred to 30% sucrose for at least 48 h. Brains were frozen and cut into 25 μm coronal sections with a cryostat. For extracellular matrix staining, fresh brains were frozen in isopentane. Sections were stored at −20 °C until staining.

Immunofluorescence

Sections were post-fixed in cold paraformaldehyde for 10 min and washed in PBS. Sections were then placed in a 0.5% Triton X-100/PBS solution for 15 min, followed by 15 min of a blocking solution (0.2% gelatin/PBS). Primary antibodies were applied for either 2 h at room temperature or overnight at 4 °C in blocking solution. The following primary antibody dilutions were used: rat anti-perlecan (1:400, clone A7L6, Chemicon, Temecula, CA), rabbit polyclonal anti-laminin (1:1000, Sigma, St Louis, MO), rabbit polyclonal anti-agrin (1:1000, kind gift of Dr. Sasaki, add his location), mouse anti-heparan sulfate (10E4 epitope, 1:400, Seikagaku Corporation, Tokyo, Japan), mouse anti-heparan sulfate (JM403 epitope, 1:400, Seikagaku Corporation, Tokyo, Japan), mouse anti-delta heparan sulfate (3G10 epitope, 1:400, Seikagaku Corporation, Tokyo, Japan), mouse anti-chondroitin sulfate (CS-56) (1:400, Abcam, Cambridge, MA), rat anti-CD133 (1:50, Chemicon, Temecula, CA), rabbit anti-GFAP (1:400, Dako, Glostrup, Denmark), mouse anti-GFAP conjugated to alexafluor 647 (1:400, Cell Signaling Tech, Boston, MA), rabbit polyclonal anti-EGF-Receptor (1:200, Chemicon, Temecula, CA), goat anti-doublecortin (DCX) (1:200, Santa Cruz Biotechnology, Santa Cruz, USA), mouse anti-NeuN (1:200, Chemicon, Temecula, CA) and rabbit anti-ssDNA (1:200, Immuno-Biological Laboratories Co, Fujioka, Gunma, Japan). Sections were then rinsed, and secondary antibodies were applied for 40 min at room temperature. The following fluorochrome-conjugated secondary antibody dilutions were used: donkey anti-mouse-CY5, donkey anti-goat-FITC (1:400, Jackson ImmunoResearch Laboratories, West Grove, USA), goat anti-rabbit alexafluor-488, and goat anti-mouse-FITC (1:400 Molecular probes, Invitrogen Corporation, Carlsbad, USA). Sections were rinsed in PBS before being treated in 2 N HCl for 30 min at 37 °C and then incubated for 10 min in a 0.1 M borate buffer (pH 8.5). Sections were rinsed before overnight incubation in rat anti-BrdU (1:800, AbD Serotec, MorphoSys AG, Planegg, Germany). Sections were rinsed and then incubated for 1 h with donkey anti-rat-CY3 (1:400, Jackson, ImmunoResearch Laboratories, West Grove, USA). Sections were rinsed and then incubated for 10 min in bis-benzimide (1:3000, Molecular Probes, Invitrogen Corporation, Carlsbad, CA). After extensive washes, sections were mounted in fluoro-gel with tris buffer (Electron Microscopy Sciences, Hatfield, USA).

Flow cytometry analysis

SVZs from 12-week-old WT-Tg and Hspg2$^{-/-}$-Tg mice ($n = 3$) were carefully dissected following the procedure described by Fischer and colleagues (Fischer et al., 2011). SVZs were then cut into small pieces and incubated for 15 min with a papain neural tissue dissociation kit from Miltenyi (Auburn, CA, USA). Cells were mechanically dissociated and passed through a 40 μm cell strainer. After washing in stain buffer (BD Bioscience, San Jose, CA, USA), the cells were incubated for 30 min in 50 μl of stain buffer with anti CD133-PE (1:20, eBioscience, San Diego, CA, USA) and with alexafluor-488-conjugated EGF (1:20, Molecular probes, Eugene, OR, USA). Cells were then fixed and permeabilized (BD Cytofix/Cytoperm kit, BD Biosciences, San Jose, CA, USA) prior to incubation with alexafluor-647 GFAP (1:40, Cell Signaling Technology, Danvers, MA, USA). Cells were washed and resuspended in 500 μl of stain buffer to perform flow cytometry analysis. The analysis was performed using a BD LSR Fortesa cell analyzer with the gate set using an appropriate isotype control.

Neurosphere culture

The cortexes of E16.5 mice were dissected and mechanically dissociated to single cell suspension. Cells were plated for 4 h to allow adherent cells to attach to the plate in DMEM/F12 and B27. Cells in suspension were recovered, counted and placed in 96 well plates at low density (300 cells/well) in 200 μl of DMEM/F12 and B27 containing EGF 20 ng/ml and different concentrations of FGF-2. Conditions were as follows: no FGF-2, control (FGF-2 20 ng/ml), and 10X FGF-2 (FGF-2 200 ng/ml). After one week in culture, the number and the size of neurospheres in each well were assessed. For differentiation, primary neurospheres were cultured for an additional 7 days on collagen-1 coated slide chambers with DMEM/F12 and 10% fetal calf serum prior to fixation in 10% PFA. Differentiated cells were then stained with GFAP, Tuj-1, and O4. Whole neurospheres were fixed in PFA (10 min) prior to immunocytochemistry as described above.

Western blotting

Whole SVZ or neurospheres were lysed in RIPA buffer (0.5% deoxycholate, 0.1% SDS, 250 mM NaCl, 25 mM Tris–HCl, pH 8, Igepal CA630, 5 mM EDTA, protease inhibitor and phosphostop; sonication 3 times 5 s). Lysates were boiled in an LDS-sample buffer (Invitrogen) with DTT for 10 min. The samples were loaded on 4–12% polyacrylamide Bis-Tris gels (Invitrogen). After electrophoresis, the proteins were transferred to a PVDF membrane (Invitrogen). The membrane was blocked with 5% skim milk in Tris-buffered saline-0.1% Tween 20, and incubated with the indicated antibodies. Primary antibodies used in Western blotting were Akt (rabbit polyclonal, Cell signaling), phospho-Akt (mouse IgG, Cell signaling), Erk1/2 (rabbit polyclonal, Cell signaling), phospho-Erk1/2 (rabbit polyclonal, Cell signaling). Secondary